CHAPTER VII

MELT FRACTURE BEHAVIOR OF NEAT AND TITANIUM DIOXIDE NANOPARTICLE-FILLED ISOTACTIC POLYPROPYLENE

ABSTRACT

The melt fracture behavior of neat isotactic polypropylene (iPP) and iPP filled with titanium dioxide (TiO_2) nanoparticles of varying content (i.e. ranging from 0 to 30 wt.%) and surface treatment (neat, silica-coated, and stearic acid-coated) during capillary extrusion was investigated by analyzing video files recorded using a high-speed CCD camera. The apparent shear rate was varied between 900 and 1800 s^{-1}. The critical shear rate at which the melt fracture was first appeared was found to increase with increasing TiO_2 content, while the severity of the melt fracture was found to increase with increasing apparent shear rate. Interestingly, at the maximum TiO_2 content of 30 wt.%, no evidence of the melt fracture was observed. At the same apparent shear rate, the severity of the melt fracture observed for iPP samples filled with stearic acid-coated TiO_2 (hydrophobic coating) was greater than that for iPP samples filled with SiO_2-coated TiO_2 (hydrophilic coating). With increasing L/D ratio (for a fixed diameter), the critical shear rate at which the melt fracture was first appeared was shifted toward a higher value and the severity of the melt fracture was less, possibly a result of the partial molecular relaxation during the flow through a longer die.

Key words: Melt fracture, polymer nano composites, Isotactic Polypropylene, Polymer extrudate.

7.1 INTRODUCTION

The process of extrusion is used to make many products, from plastic bags to textile fibers. One limitation of production rate is the flow instability phenomenon occurring when polymer extrudate at rate exceeding a critical shear stress. It is called melt fracture. The occurrence of melt fracture is very important industrial problem because it is taken to effect of physical, optical, aesthetical properties of the product. There are two types of theories to explain the mechanism of melt instability. One is based on the slip-stick at the die wall, and another based on the periodic growth at relaxation of tensile stress at the extrudate surface at the die exit [1-7]. Many well known methods to suppress the melt instability by several researchers, for instance, increasing the melt temperature [8]; decreasing only the die temperature [9,10]; broadening of molecular weight distribution [11]; adding the external lubricant in the resin [12-13]. The observation of frequency or wave length of PP after die exit has been rarely reported. Under large shear stress further instability of difference characters on the solidified extrudate. In particular, a relationship between the shear stress and extrudate behavior are very interesting. Fujiyama and Inata [8] investigated the melt fracture behavior of PP in various types of narrow molecular weight distribution and additive of adhesive resins. They were found that the controlled-rheology PP and PP-type thermoplastic elastomer with narrow molecular weight distributions easily generate the sharkskin and melt fracture originating at the die exit, from a shear rate nearly one decade lower than rates of elastic failure of homo-PP and block-PP. Moreover, the critical shear rate which sharkskin occurs increases with increasing extrusion temperature. Tao and Huang [14] observed melt fracture of PP resins in case of the relationship between frequency wave length and the given shear rate. The results showed that the frequency increased when molecular weight decreased and when temperature increased.

In which focus on rheological properties of the polymer composites, are characterized by the evolution of the structure of the dispersion and distribution in the melt flow. The composites system displays a rather complex rheological behavior both of dispersed phase and continuous phase [15]. The influence of inorganic fillers on rheological behavior usually showed as solid like behavior. Also filler particles,

particularly those in nano scale, had noticeable effect on the movement of polymer molecules [16]. However, the apparent melt fracture and the dispersion of the filler agglomerates have not yet been studied. Recently, Hatzikiakos et al. [17] studied on the effect of processing additive nanoclays on the rheological properties of PP.They found that the presence of small a mount of nanoclays on their processibility can be easily dispersed in to the matrix and can not only eliminate the onset of sharkskin melt fracture but may significantly pospond the onset of melt fracture to much higher rates.

In this article, the real time melt fracture and rheological behavior of the PP filled TiO_2 nano particles were studied in following wall shear stress. In subsequent discussion, it was revealed that the effect of coating surface of nano particle on apparent melt fracture.

7.2 EXPERIMENTAL DETAILS

Materials

The general purpose PP homopolymer resin used as matrix polymer component include Polypropylene (PP) HP 400K was supplied by HMC Polymers Co., Ltd (Rayong Thailand) [18]. Specific properties of the resin, provide by ASTM and DIN standard for laboratory, are as follows, MFR (2.16kg at 190°C)= 4, density= 0.9 gcm^{-3}, tensile strength at yield= 33 nmm^{-2}, elongation at yield = 10%, flexural modulus = 1400 MPa, and notched izod impact strength at 23 °C = 30. Three types of TiO_2 nanoparticles were supplied by Advanced Nanotechnology Co., Ltd. (Samutprakarn Thailand) [19]. All of nano materials have an excellent properties as average particle size = 55 nm, specific surface area = 35 m^3/g, pH = 6-8. The different of three types are surface properties. CYU 201 and CYU 202 have a hydrophilic surface (non treated surface and Sio_2 treated surface, respectively). Another one, CYU 203 has a hydrophobic surface as stearic acid treatment.

Compounding

TiO_2 nanoparticles were dried in an oven at 80°C for 24 h and then pre-mixed with iPP pellets in a tumble mixer for 20 min in various compositional ratios (i.e. 5, 10, 20, and 30 wt%). The compounding were then fed in to COLLIN ZK25 self wiping, co-rotating twin screw extruder operated at a screw speed of 80 rpm and temperature profile of 185°C (die zone), 190°C (zone 5), 185°C (zone 4), 180°C (zone 3), 175°C (zone 2), and 100°C (feed zone). The extrudate was rapid cooled in water bath and cut into pellet form by a Planetrol 075 de pelletizer.

Rheological measurements and imaging melt fracture behavior.

Capillary rheometer (CEAST Rheologic 5000 twin bore capillary rheometer) was used to generate in various apparent shear rate. The dimensions of instrument was 15 and 300 mm diameter and length of the barrel, L/D ratio of die series as 10/2 and 30/2, respectively, the testing temperature was set on 190 °C $\pm$ 0.5°C and the hold on time and hold on pressure for stages 1, 2, and 3 were 230 sec and 10, 20 and 30 Pa, respectively.

Imaging melt fracture photo

A CCD direct camera (FUJIKO FK2275 color camera 1/4) has been set up after the die exit to image the extrudate. It is connected with a converter box (AVER MEDIA M026 high speed USB 2.0) to generate digital signal. The signal was analyzed by a micro computer. The semAfor software was used to measure the dimension of shapes. The measurement dimension was shown on fig. 7.1. The frequency was calculated using the following equation:

$$\nu = \langle V \rangle / \lambda = \dot{\gamma}^{o} / D / wavelength \times D_{ex} / (D_{ex} / D)^2 / (\rho_{25} / \rho T) \qquad (7.1)$$

where $<V>$ is the average velocity at the die exit, λ is the wave length measured at the die exit, D_{ex} is the diameter of solid extrudate, D is the diameter of die, $\dot{\gamma}^{o}$ is apparent shear rate, and $\rho_{25} / \rho T$ is the density ratio to reflect the actual wave length at the die exit [20].

7.3 RESULTS AND DISCUSSION

Typical severity of melt fracture images in the whole range recorded at various shear rate of neat PP, 5 wt%, and 30 wt% are shown in fig. 7.2. It can be seen that the neat PP exhibited the onset of melt fracture from 900 ^{o}C to 1800 ^{o}C. With increasing in the amount of fillers, the melt fracture tended to decrease and disappeared on maximum fillers at 30 wt%. The apparent melt fractures of neat PP at different shear rates are shown on fig. 7.3. It provided more evidence the severity onset of melt fracture is measurable. The image of CYU 203 series depicted in fig. 7.4 showed that the different characteristics of CYU 203 composites at various amount of fillers from 5 wt% to 30 wt%. The results significantly showed the more the fillers added the less the fracture behavior observed. Moreover, it completely developed at 30 wt% of filler. It can imply that the nano TiO_2 particles as a fillers have more effect on the movement of polymer molecular chains. In terms of the effect of L/D ratio, CYU 203 series has been illustrated in fig. 7.5. As longer die used, the significant decrease in the onset of melt fracture and the dimension were observed. On the other hand, all images showed previously depicted only the basic different of the fracture. Then, the results and discussion on the detail of shape were analyzed as follow.

The frequency of fracture as a function of apparent shear rate for neat PP and 5 wt% of fillers are plotted in fig. 7.6. Neat PP exhibited greater frequency than other composites. Also, it increased with increasing apparent shear rate. Furthermore, all of 5 wt% composites slightly increased because an applied apparent shear rate rises up shear stress on the system. Then, it is released after passing through the capillary die known as "stress relaxation". The frequency directly affected on release stress. So the reduction of frequency value of 5 wt% composites compared to the neat PP could be explained in terms of the movement of molecules shown in the previous work [21]. The nano particle would block the chain movement and created the inner free volume confirmed by the DSC curve on the results of the author [16]. They suggested that the difference in Tg of TiO_2 nano particles filled in HIPS provided sufficient to looking for the inner free volume. Fig.

7.7 showed the effect on amount of TiO_2 nano fillers on apparent shear rate of CYU 203 type. The greater amounts of filler tend to reduce the frequency fracture and the lowest value was obtained at 20 wt% of filler. Moreover, no melt fracture took placed at 30 wt%. This result means that an influence of nano TiO_2 particles on the composites can be delayed the onset of melt fracture at the same rate. The other type of fillers presented similarly behavior. The fig. 7.8 showed effect of 3 types of filler at 1800 s^{-1} of shear rate. The suppressive effect of coating surface was more remarkably observed at low loading of nano particles, such as, 5 and 10 wt%. The frequency of iPP sample filled with stearic acid coated TiO_2 (hydrophobic coating), CYU 203, was greater than those of iPP sample filled with SiO_2 coated TiO_2 (hydrophilic coating), CYU 202, and without surface coating on CYU 201. However, all of them collapsed at high loading of filling at 20 wt% of filler. These results showed more evidence and supported on the previous work on severity of flow curve and extruded swell on the same type composite [22] . It was suggested that the hydrophobic surface coating has less effect on the molecular relaxation compared to the hydrophilic surface due to the better dispersive and distribution on the iPP matrix. The effect of die length is shown on Fig 7.9. Both line graphs presented the reduction of frequency as a function of amount of fillers on 1800 s^{-1} of CYU 203 composites. The increase in path line of melt flow also improved the resident time of system leading to greater partial molecular relaxation. So, the longer die used appeared to reduce the frequency.

The real dimensions of fracture can be measured and compared. Dependence of frequency width on apparent shear rate for neat and 5 wt% of composites is explained in fig 7.10. All composites had greater width than neat iPP. Neat iPP does not provide much increase in frequency as the shear rate increase. There were not absolute results on the effect of surface coating. However, in case of high shear rate (1600-1800 s^{-1}), the hydrophobic surface treatment TiO_2 nanoparticle exhibited the closer frequency width to the value of iPP compared to the hydrophilic surface treatment. On the other hand, the frequency length as a function of the apparent shear rate for neat iPP and 5 wt% of fillers is also reported on fig. 7.11. Generally, neat iPP exhibited no much difference in frequency length as the shear rate increase. Nevertheless, in case of composites, significant increases in the

frequency width were observed as the applying apparent shear rate increase. Therefore, the nano TiO_2 particles mainly affected on the severity fracture shape. The length and width of fracture has been changed not only the applied shear stress, but also depended on the movement of molecular relaxation. Nano TiO_2 can be generated the free volume and block the relaxation of polymer chains so the frequency width and length could be greater. Fig 7.12 and fig 7.13 showed the effect of amount of filler on apparent shear rate for neat iPP and CYU 203. The results exhibited that the higher the filler loaded, the greater the frequency width and length obtained. With increasing the apparent shear rate, neat PP did not show much difference in frequency width (see fig 7.12). For the lower amount of filler loaded, 5 and 10 wt%, there were significant reductions at high shear rate. This is due to the fact that the agglomeration of nano TiO_2 would be broken apart leading to the reduction in the inner free volume. Also, it efficiently blocked the movement of polymer chains. However, the frequency width remained unchanged for 20 wt% of filler loading because there were more content of secondary phase on the matrix phase leading to incomplete breaking apart at the high amount of filler. At the same time, the frequency length exhibited analogous behavior shown in fig 7.13. The apparent shear rate provided the positive effect on the frequency length of 5 and 10 wt% fillers loading samples. However, the effect of shear rate on the frequency length at 20 wt% was not obvious. The effect of TiO_2 types are depicted fig 7.14 and fig 7.15. It can be seen that the frequency width was strongly affected by the filler loading as shown in fig 7.14. The hydrophilic types (CYU 201 and CYU 202) provided the higher value than another hydrophobic (CYU 203). This is attributed to the dispersion and distribution of the filler resulting in the fracture shape. As for the frequency length concerned (see fig. 7.15), all of iPP filled TiO_2 tested did not show much difference compared to the frequency width. It may be concluded that the first normal stress differences in the flow part line direction is much higher than secondary stress differences [23]. Moreover, the melt velocity in the radial direction was smaller than that in the axial and lateral directions [24]. So, the molecular relaxation takes place on the cross direction. The results in fig 7.16 showed the effect of die dimension on the frequency width. It strongly supported the previous result on frequency as a function of fillers. The results also suggested that with increasing a

die length, the frequency width decreased, while the frequency length increased. So the residence time is one of factors to control the fracture behavior of the TiO_2 nano composites.

Fig 7.17 and 7.18 showed the results of twist angle on apparent shear rate. The results confirmed that the TiO_2 nanofillers have the effect on fracture behavior. All of composites provided greater angle of twist than neat iPP did. The hydrophilic surface of fillers influenced to the twist angle by increasing the apparent share rate leading to higher twist angle compared to the hydrophobic surface. Moreover, the results in fig 7.18 exhibited that the twist angle increased with increasing amount of fillers.

7.4 CONCLUSION

The melt fracture phenomenon was observed by the addition of TiO_2 nanoparticles in iPP matrix at various filler loading, ranging from 5 to 30 wt% during capillary extrusion process. In the whole range of the shear rate studied, the frequency of all samples tested increased with increasing applied apparent shear rate. However, the frequency decreased as the amount of nanoparticles filled from 0 to 20 wt% while the frequency completely developed on 30 wt%. The nano TiO_2 particles as fillers have more effect on polymer molecular chains movement. Moreover, the nano TiO_2 particles on the composites would delay the onset of melt fracture as the same shear rate. The surface coating on nano particles also resulted in the severity of melt fracture. By applying the same shear rate, the hydrophobic surface TiO_2 particles exhibited greater frequency than hydrophilic surface coating due to the better dispersive and distribution on the iPP matrix. As for typical frequency length and frequency width at various shear rates, it can be seen that both increased as more amount of fillers added. The results on twist angle exhibited non-linearly manner at a given apparent shear rate. At the same time, the largest twist angle was on the maximum at 20 wt%. All of the results suggested that the introduction of the nano fillers could induce the increase in inner free volume and the effect elastic chains movement could be blocked leading to the change in the severity of melt fracture. In

addition, the melt fracture phenomenon also depended on the die dimension, such as, die length. The longer the die used, the less the melt fracture took place.

7.5 ACKNOWLEDGMENTS

The authors would like to acknowledge the Asahi Glass Foundation on Overseas Research Grant for financial supported. Partial supports received from the Petroleum and Petrochemical Technology Consortium (through a governmental loan from the Asian Development Bank) and from the Petroleum and Petrochemical College, Chulalongkorn University are gratefully acknowledged.

7.6 REFERENCES

[1] J. D. Shore, D. Ronis, L. Piche, M. Grant, Physical Review, 55 (1997) 2976.

[2] M. D. Graham, Chaos 9 (1999) 154.

[3] J. D. Shore, D. Ronis, L. Piche, M. Grant, Physical Review Letters, 77 (1996) 655.

[4] B. Meulenbroek, C. Storm, V. Bertola, C. Wagner, D. Bonn, W. V. Saarloos, Physical Review Letters, 90 (2003) 024502.

[5] S. Kim, J. M. Dealy, Polymer Engineering and Science 42(2002) 482.

[6] D. M. Kalyon, H. Gevgilili, Journal of Rheology 47(2003) 683.

[7] R. D. Chien, W. R. Jong, S. C. Chen, Journal of Micromechanics and Microengineering 15 (2005) 1389.

[8] M. Fujiyama, H. Inata, Journal of Applied Polymer Science 84 (2002) 2111.

[9] O. Kulikov, K. Hornung, Journal of Non Newtonian Fluid Mechanics 124 (2004) 103.

[10] Y. Goutille, J. guillet, Journal of Non Newtonian Fluid Mechanics 102 (2002) 19.

[11] J. J. Baik, C. Tzoganakis, Polymer Engineering and Science 38 (1998) 274.

[12] Y. C. Kim, K. S. Yang, C. H. Choi, Journal of Applied Polymer Science 70 (1998) 2187.

[13] M. Fujiyama, H. Inata, Journal of Applied Polymer Science 84 (2002) 2120.

[14] Z. Tao, J C. Huang, Polymer 44 (2003) 719.

[15] A. Hamamoto, T. Tanaka, Journal of Vinyl & Additive Technology 6 (2000) 20.

[16] X. Wang, Z. Wang, Q. Wu, Journal of Applied Polymer Science 96 (2005) 802.

[17] S. G. Hatzikiriakos, N. Rathod, E. B. Muliawan, Polymer Engineering and Science (2005) 1098.

[18] Available from http://www.hmcpolymer.com/products/Homo_/HP-400_files.

[19] Available from http://www.advnano.com/products

[20] P. Zoller, D. J. Wash, Standard Pressure-Volume-Temperature data for polymers, CRC press (1995) 47.

[21] R. Dangtungee, J. Yun, P. Su paphol, Polymer Testing 24(2005) 2.

[22] R. Dangtungee, P. Su paphol, Observation of rheological properties and extrudate swell of iPP-TiO_2 nanocomposites. (In progress).

[23] Y. Hori, S. Okubo, Journal of Rheology 24(1980) 39.

[24] Y. Son, K. B. Migler, Journal of polymer Science Part B: Polymer Physics 40(2002) 2791.

7.7 LIST OF FIGURES

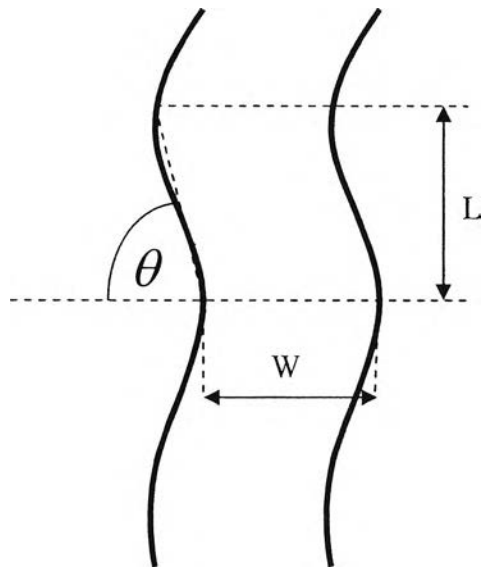

Fig. 7.1

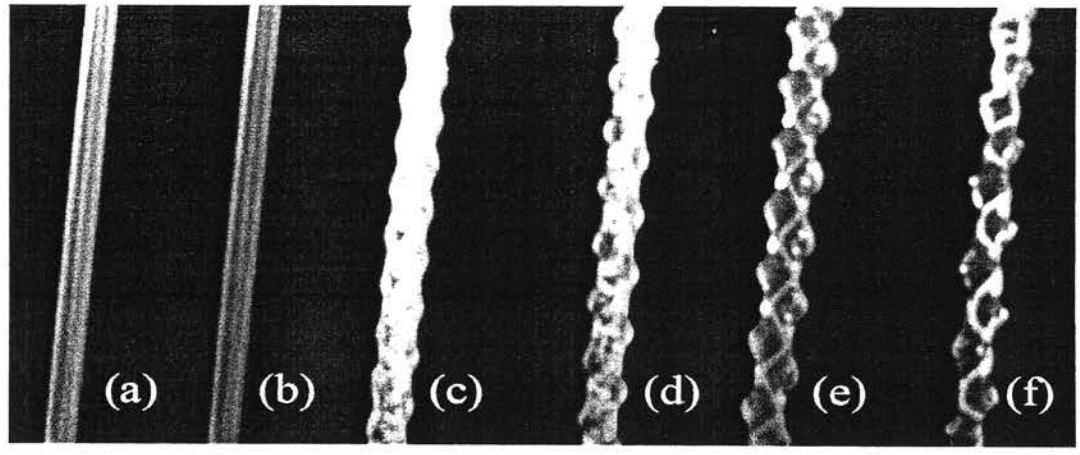

Neat PP

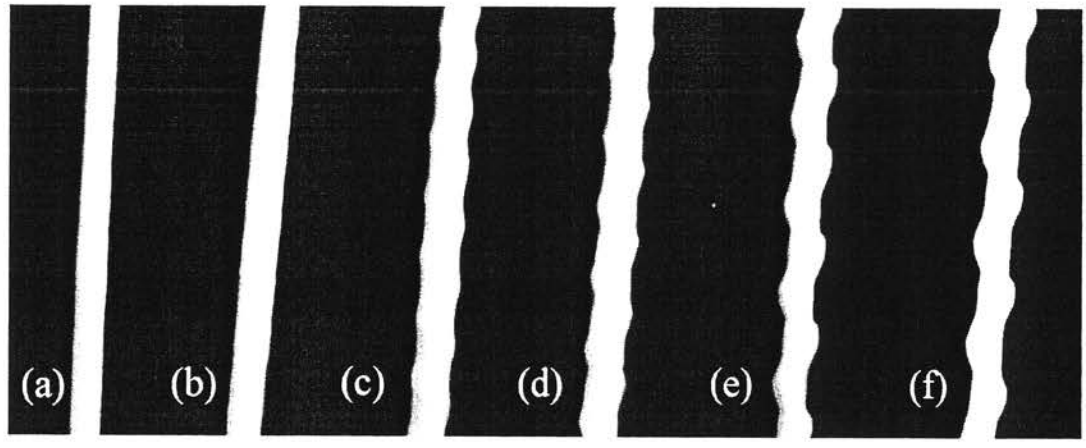

5 wt% CYU 203

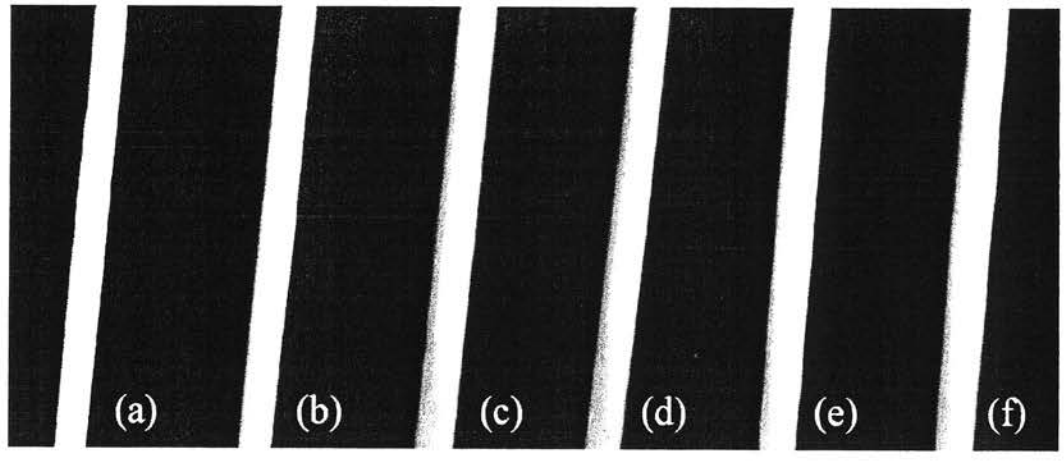

30 wt% CYU 203

Fig. 7.2

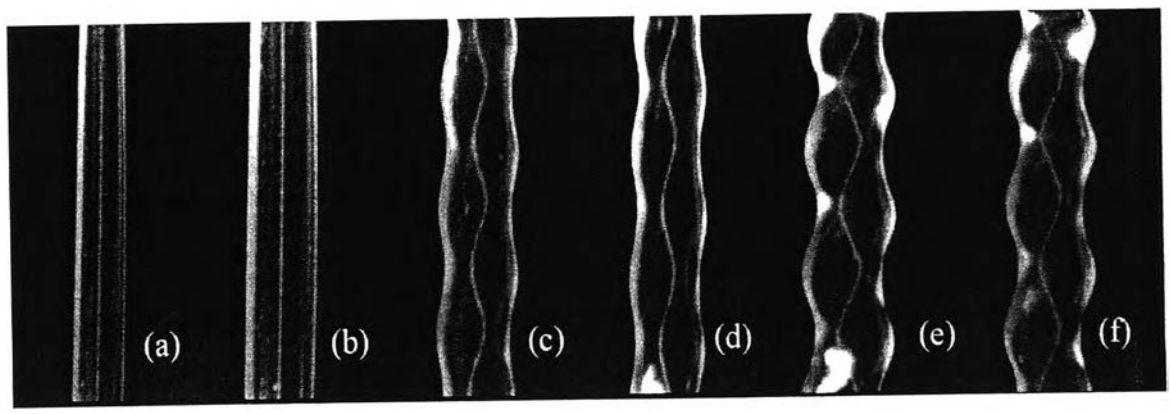

Fig. 7.3

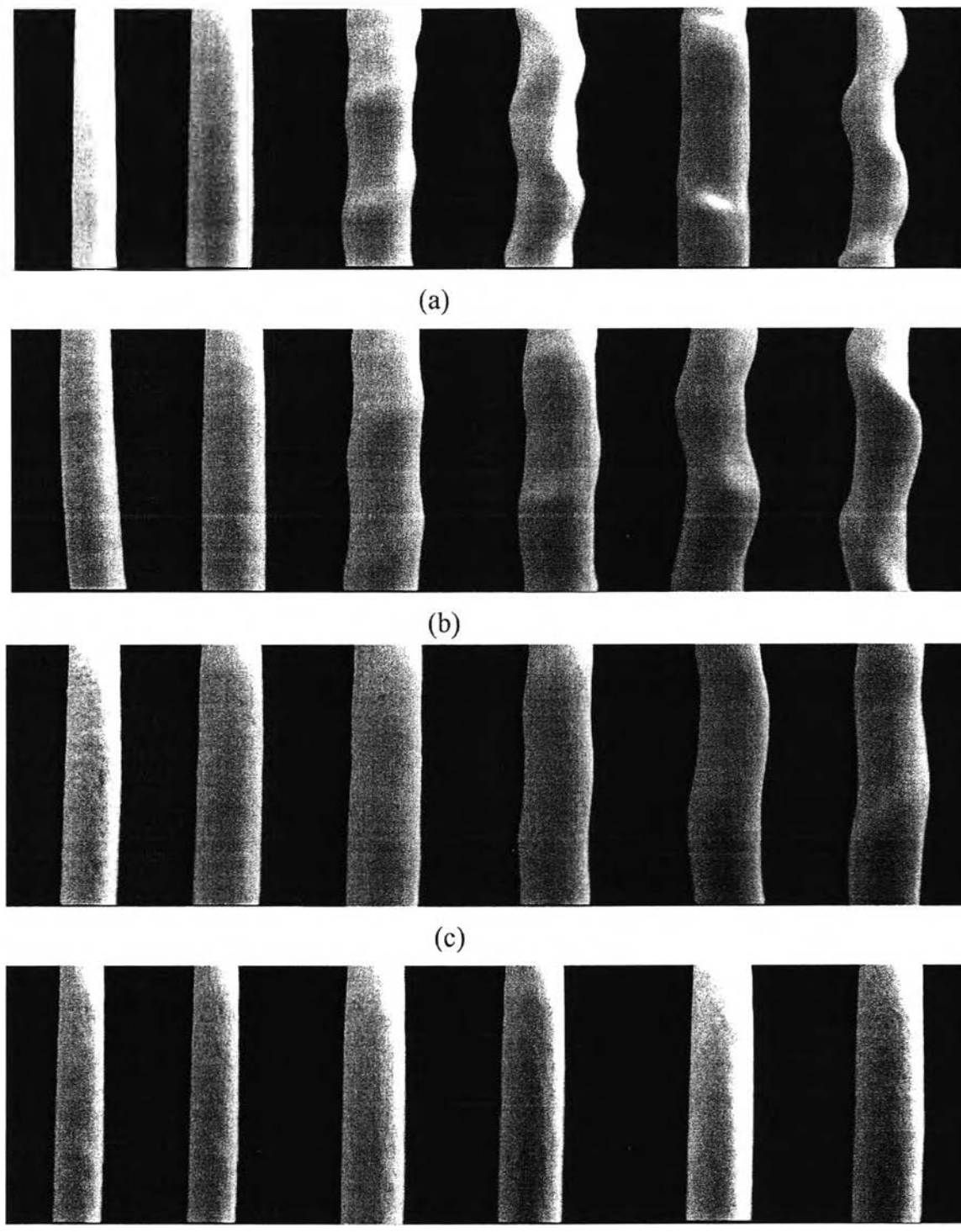

Fig. 7.4

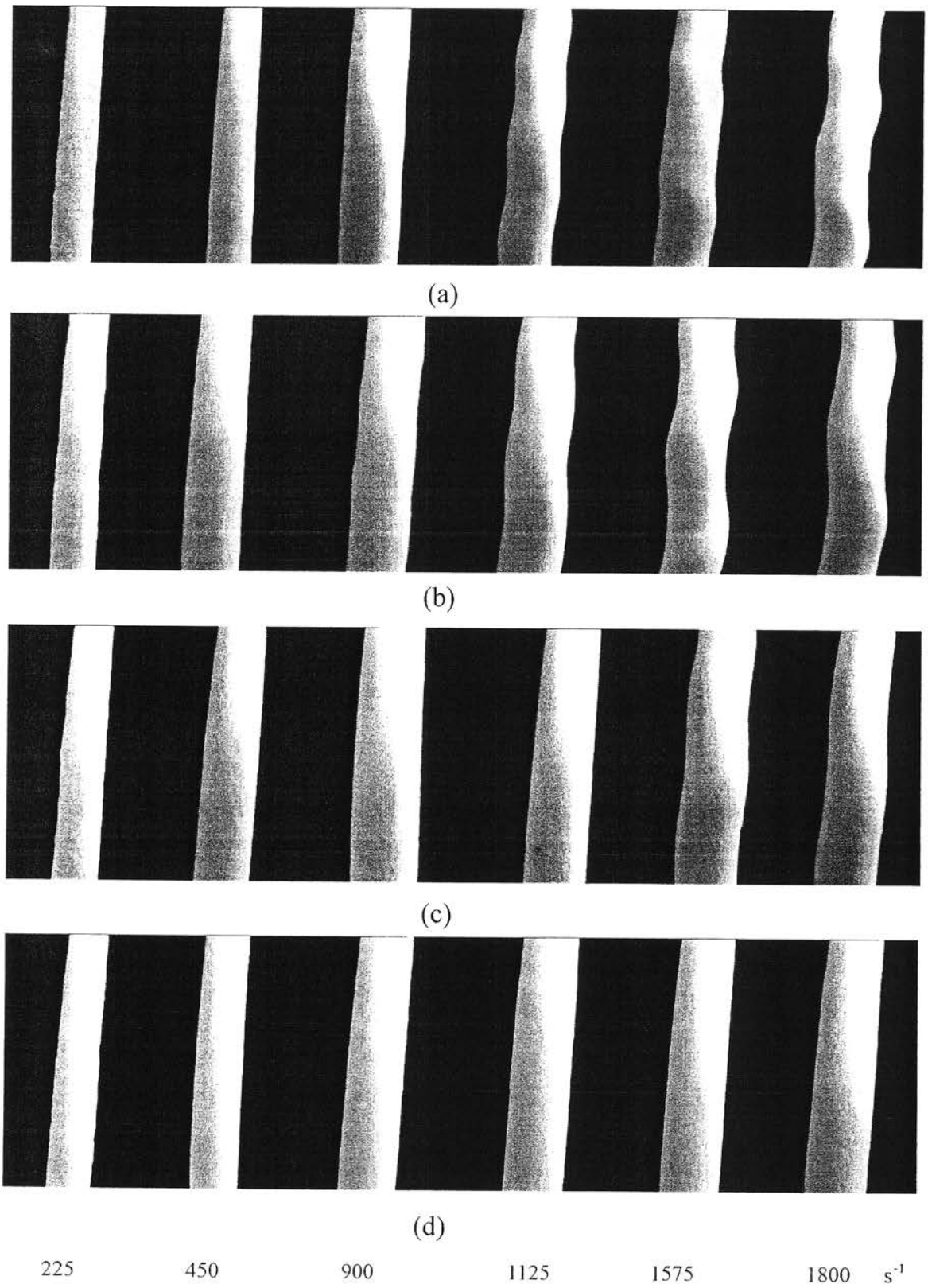

Fig. 7.5

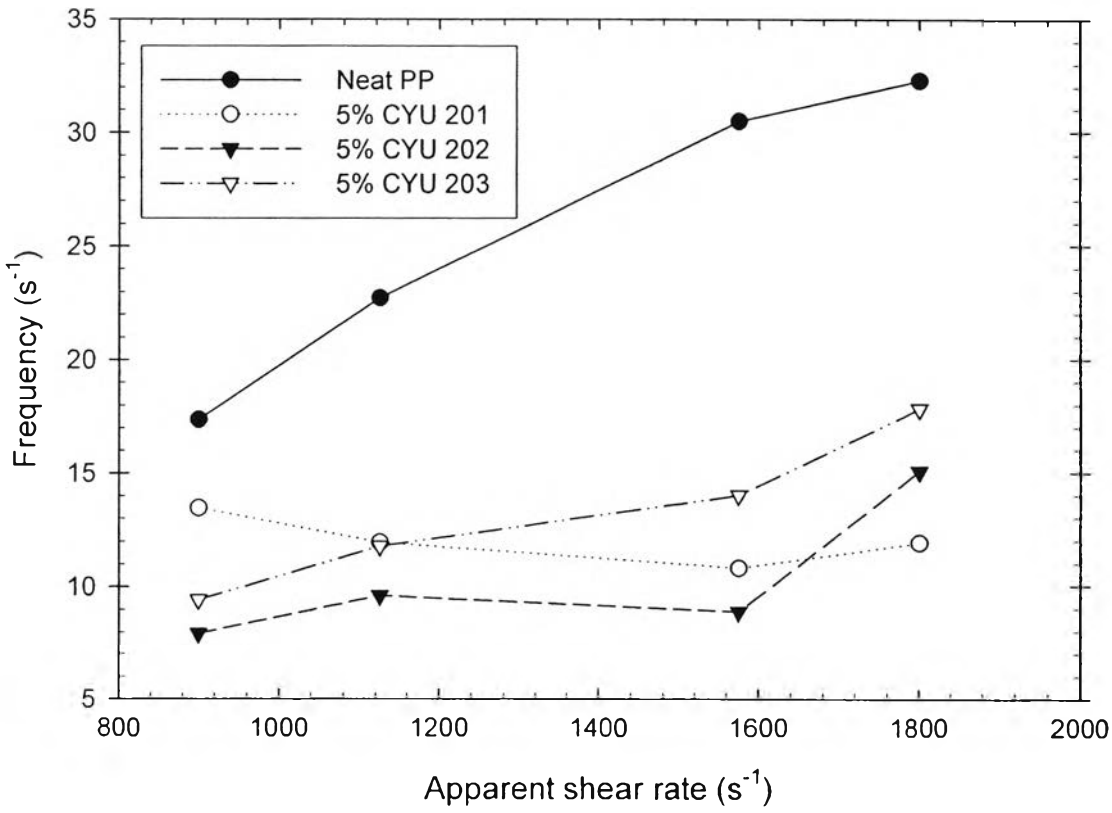
Neat PP
5% CYU 201
5% CYU 202
5% CYU 203
Frequency (s^{-1})
Apparent shear rate (s^{-1})
35
30
25
20
15
10
5
800
1000
1200
1400
1600
1800
2000

Fig. 7.6

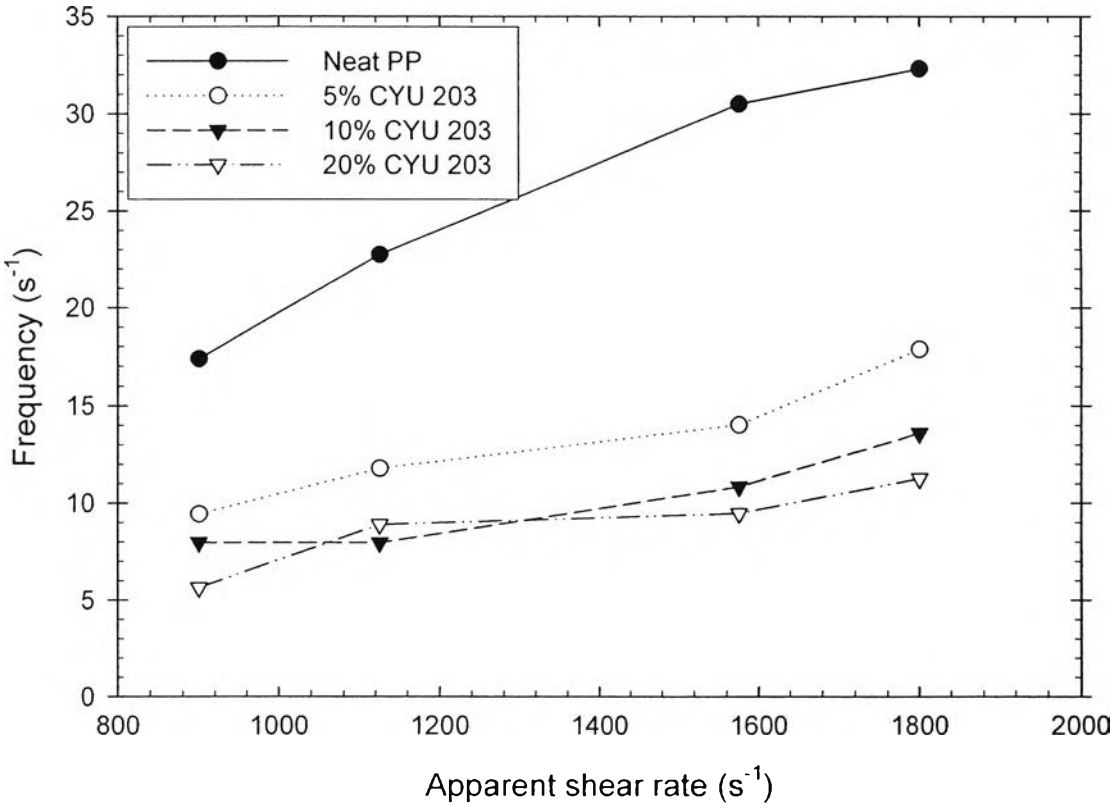
Neat PP
5% CYU 203
10% CYU 203
20% CYU 203
Frequency (s-1)
Apparent shear rate (s-1)
0
5
10
15
20
25
30
35
800
1000
1200
1400
1600
1800
2000

Fig. 7.7

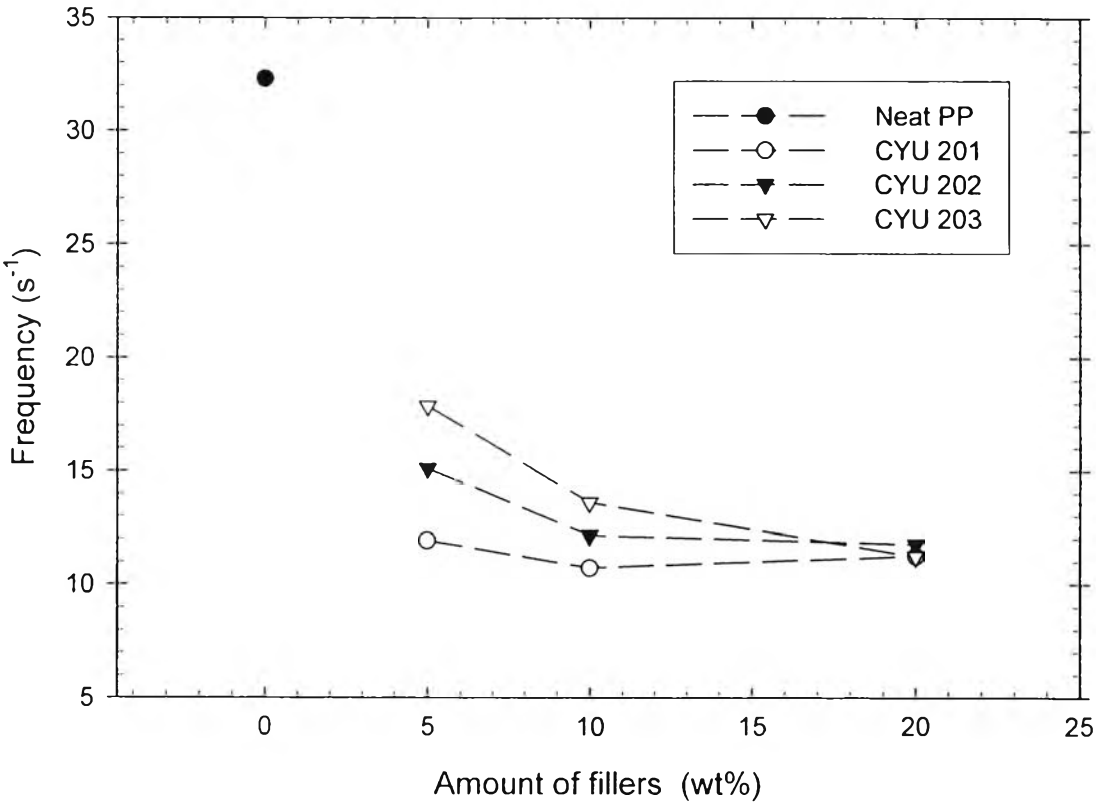
35
30
25
20
15
10
5
Frequency (s-1)
0
5
10
15
20
25
Amount of fillers (wt%)
Neat PP
CYU 201
CYU 202
CYU 203

Fig. 7.8

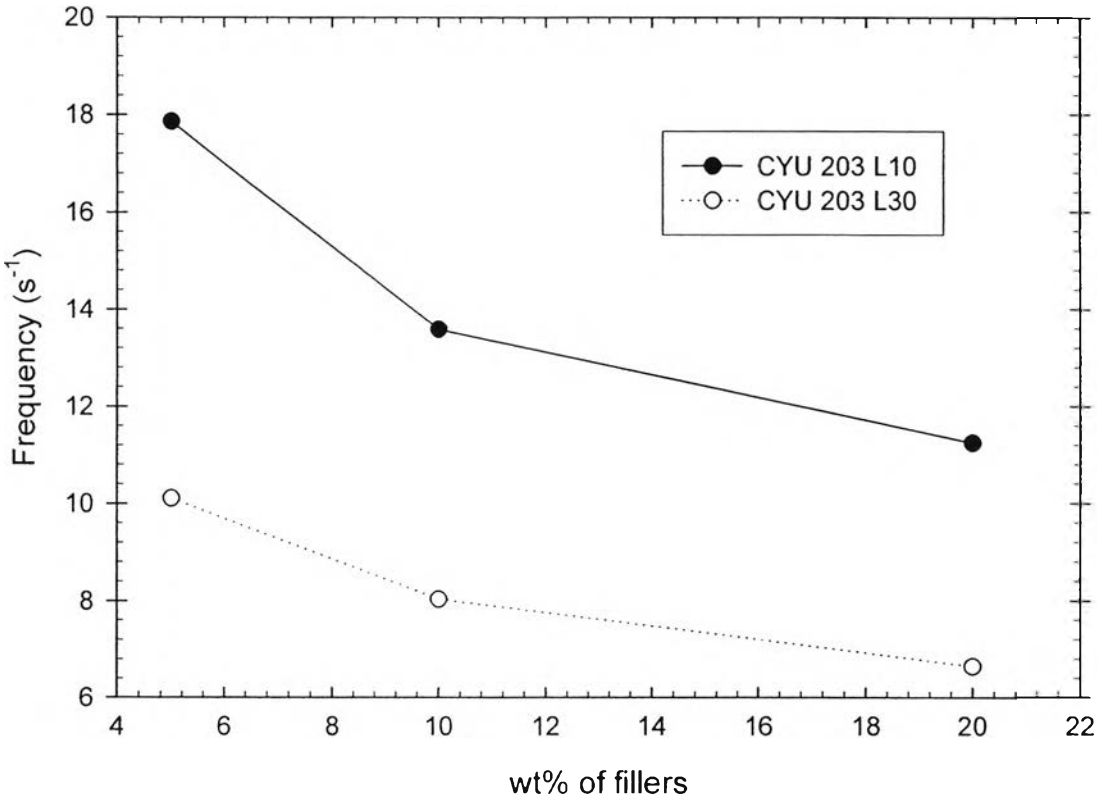
20
18
16
14
12
10
8
6
4
6
8
10
12
14
16
18
20
22
Frequency (s-1)
wt% of fillers
CYU 203 L10
CYU 203 L30

Fig. 7.9

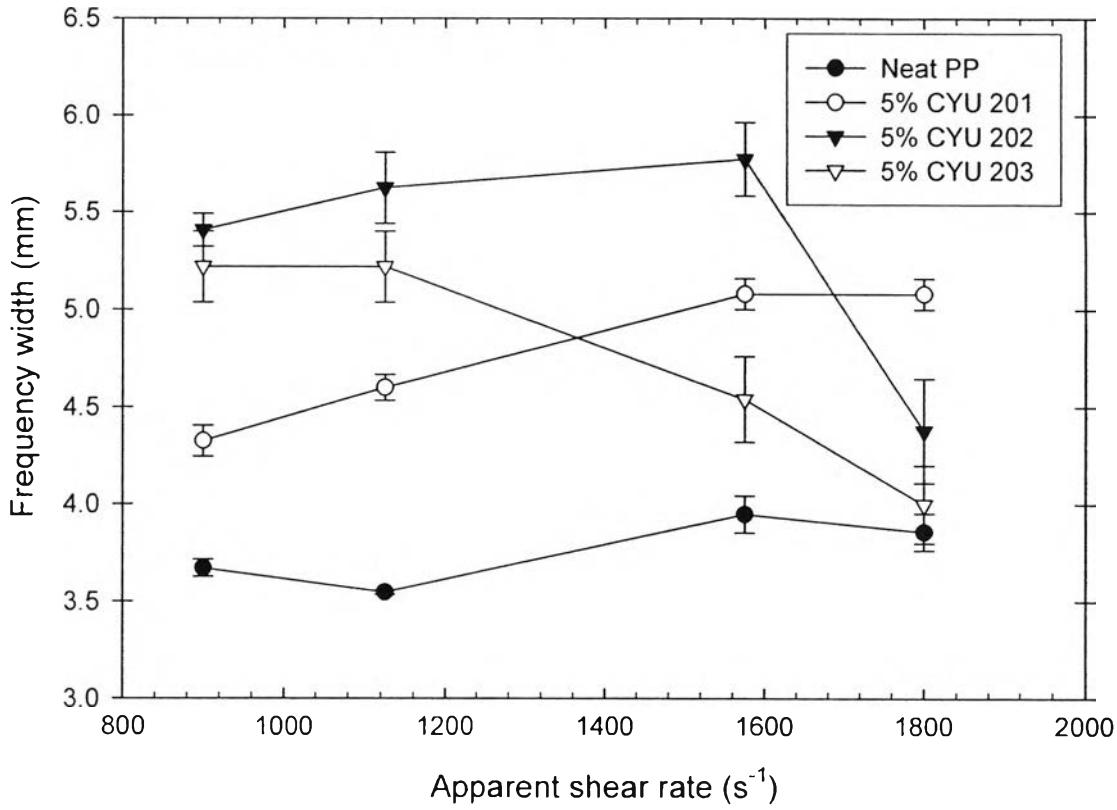
Neat PP
5% CYU 201
5% CYU 202
5% CYU 203
Frequency width (mm)
Apparent shear rate (s-1)
6.5
6.0
5.5
5.0
4.5
4.0
3.5
3.0
800
1000
1200
1400
1600
1800
2000

Fig. 7.10

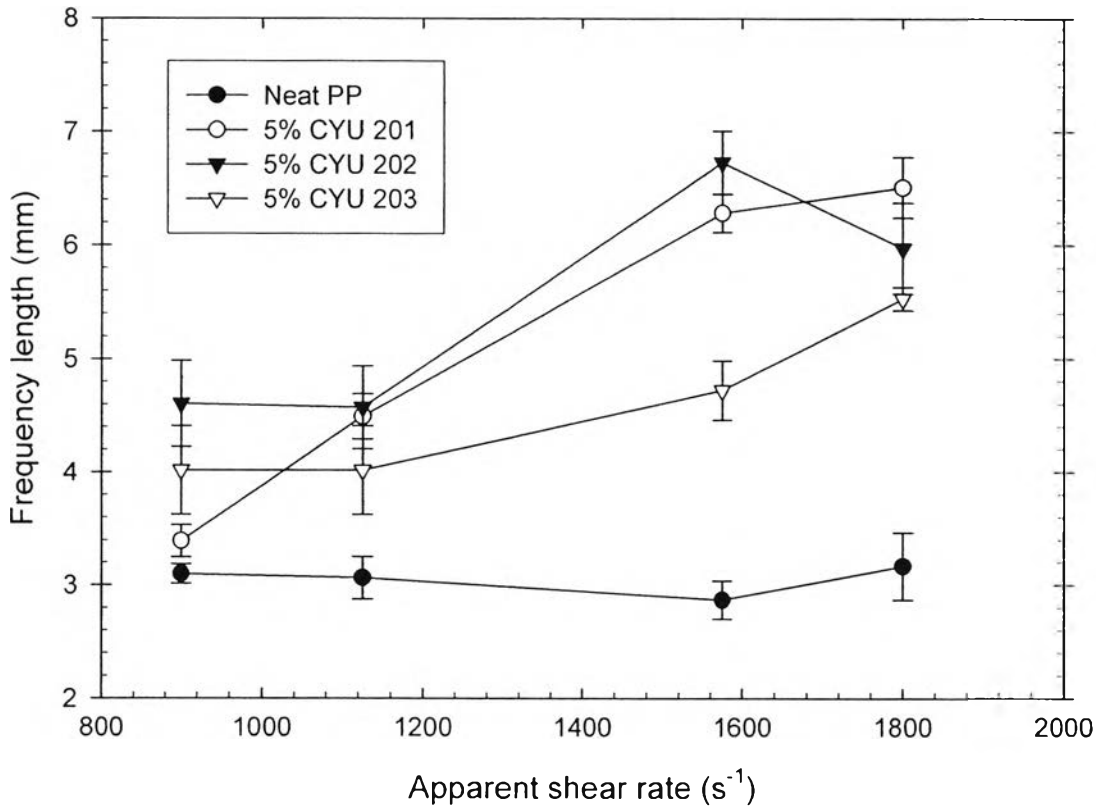
Neat PP
5% CYU 201
5% CYU 202
5% CYU 203
Frequency length (mm)
Apparent shear rate (s-1)
2
3
4
5
6
7
8
800
1000
1200
1400
1600
1800
2000

Fig. 7.11

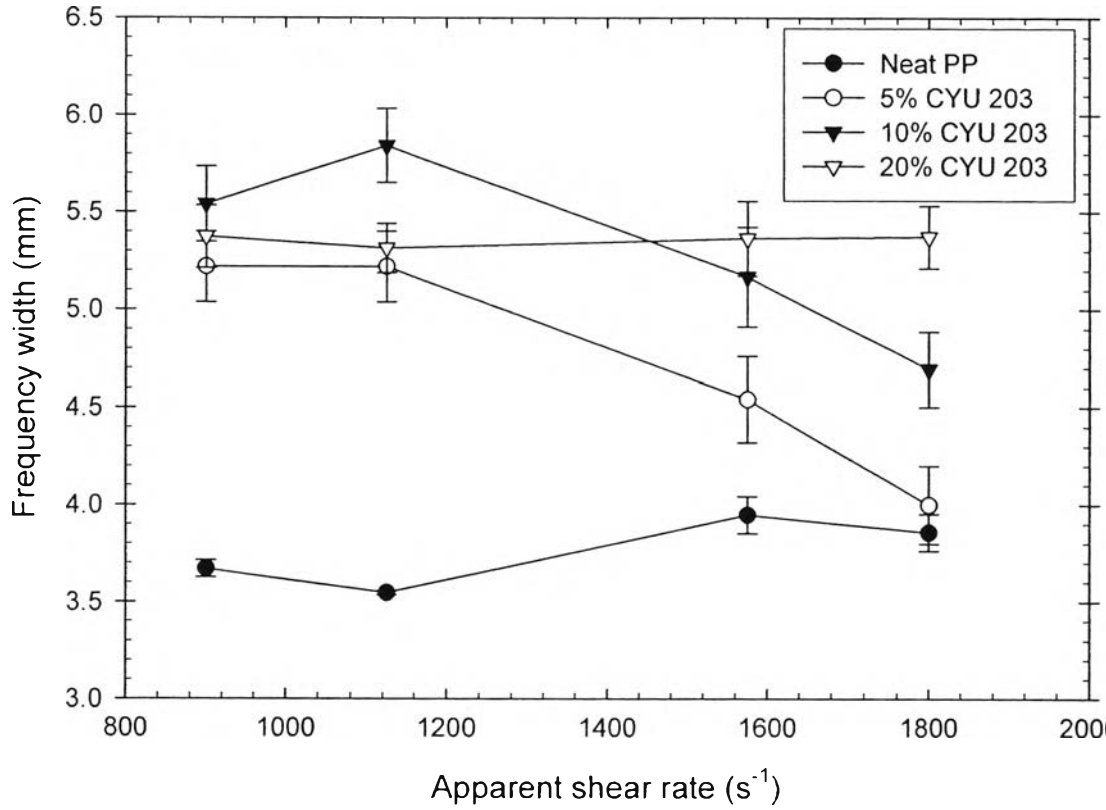
Neat PP
5% CYU 203
10% CYU 203
20% CYU 203
Frequency width (mm)
Apparent shear rate (s-1)
6.5
6.0
5.5
5.0
4.5
4.0
3.5
3.0
800
1000
1200
1400
1600
1800
2000

Fig. 7.12

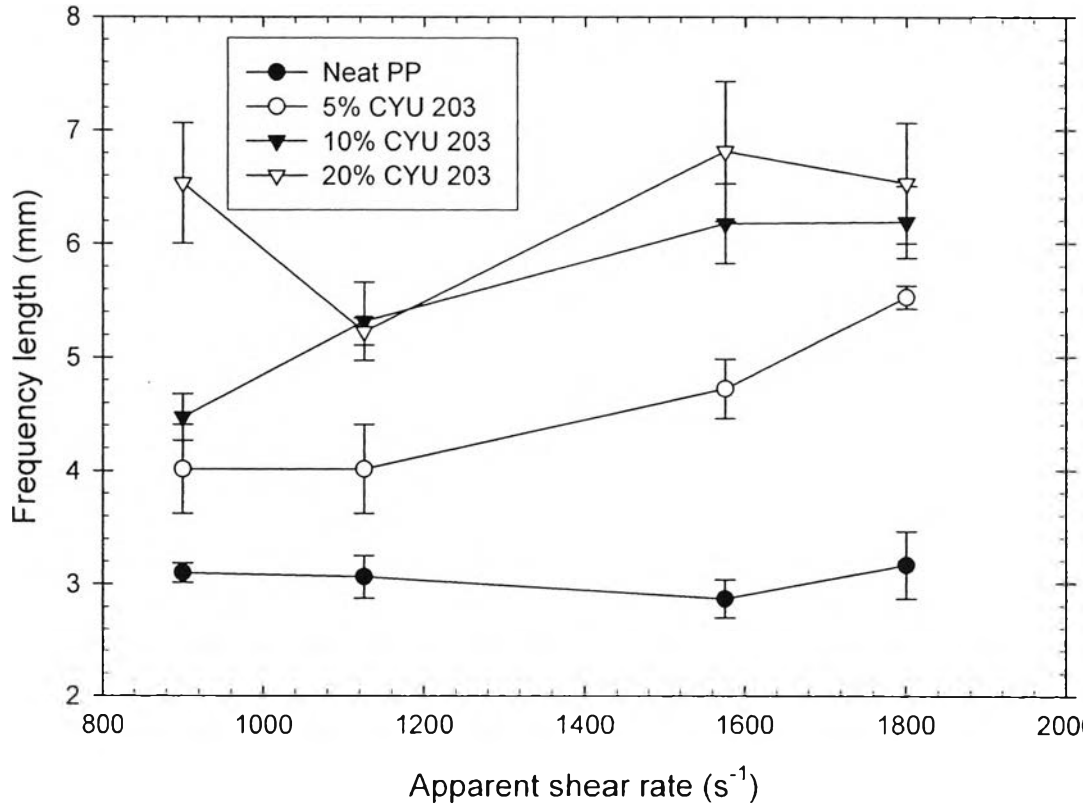
Neat PP
5% CYU 203
10% CYU 203
20% CYU 203
Frequency length (mm)
Apparent shear rate (s-1)
2
3
4
5
6
7
8
800
1000
1200
1400
1600
1800
2000

Fig. 7.13

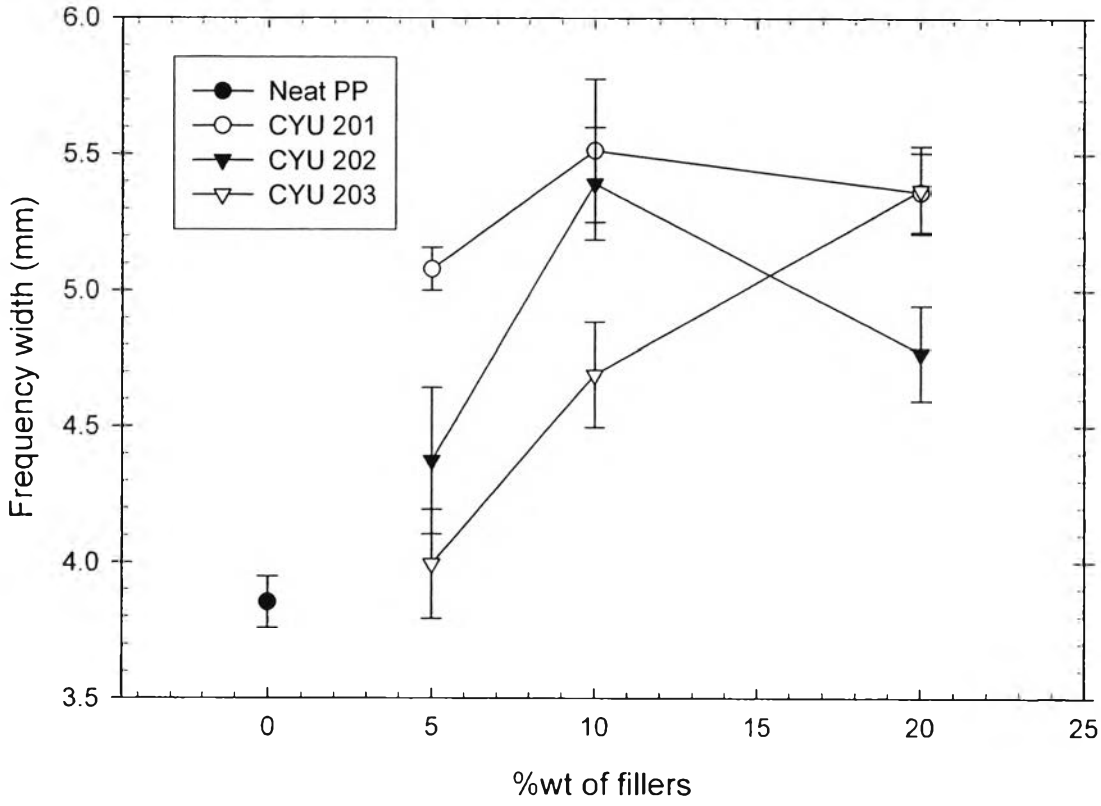
Neat PP
CYU 201
CYU 202
CYU 203
Frequency width (mm)
%wt of fillers
6.0
5.5
5.0
4.5
4.0
3.5
0
5
10
15
20
25

Fig. 7.14

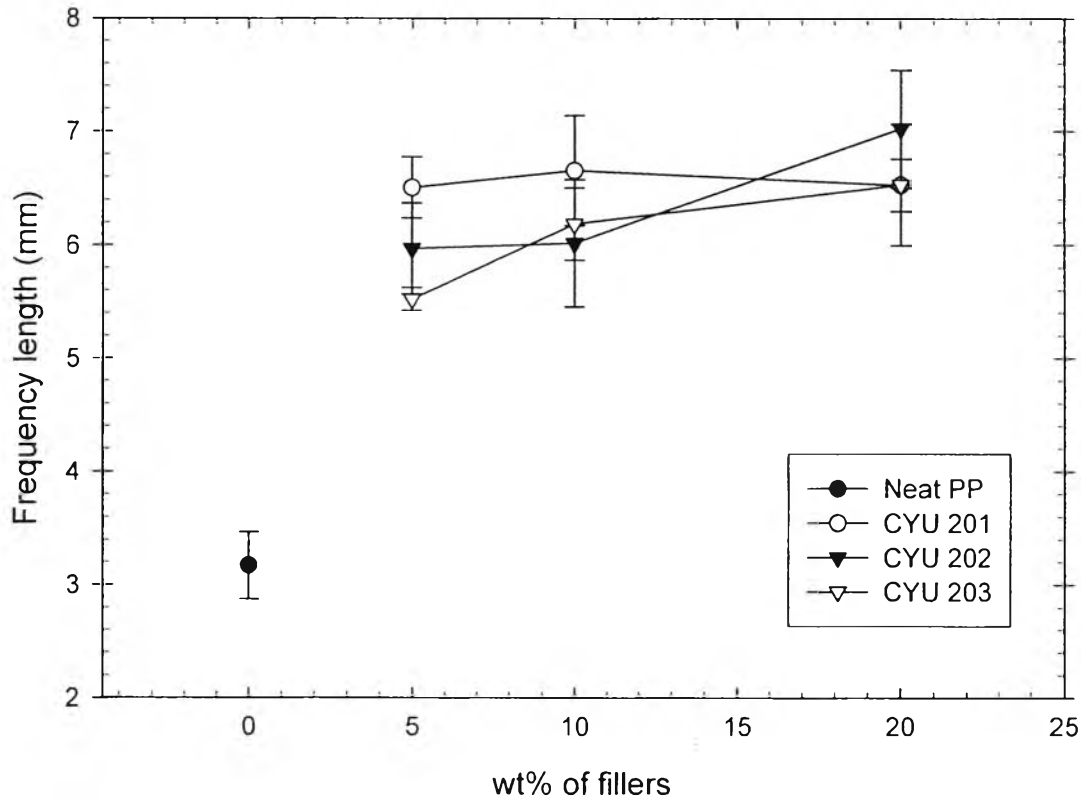
Frequency length (mm)
wt% of fillers
Neat PP
CYU 201
CYU 202
CYU 203
2
3
4
5
6
7
8
0
5
10
15
20
25

Fig. 7.15

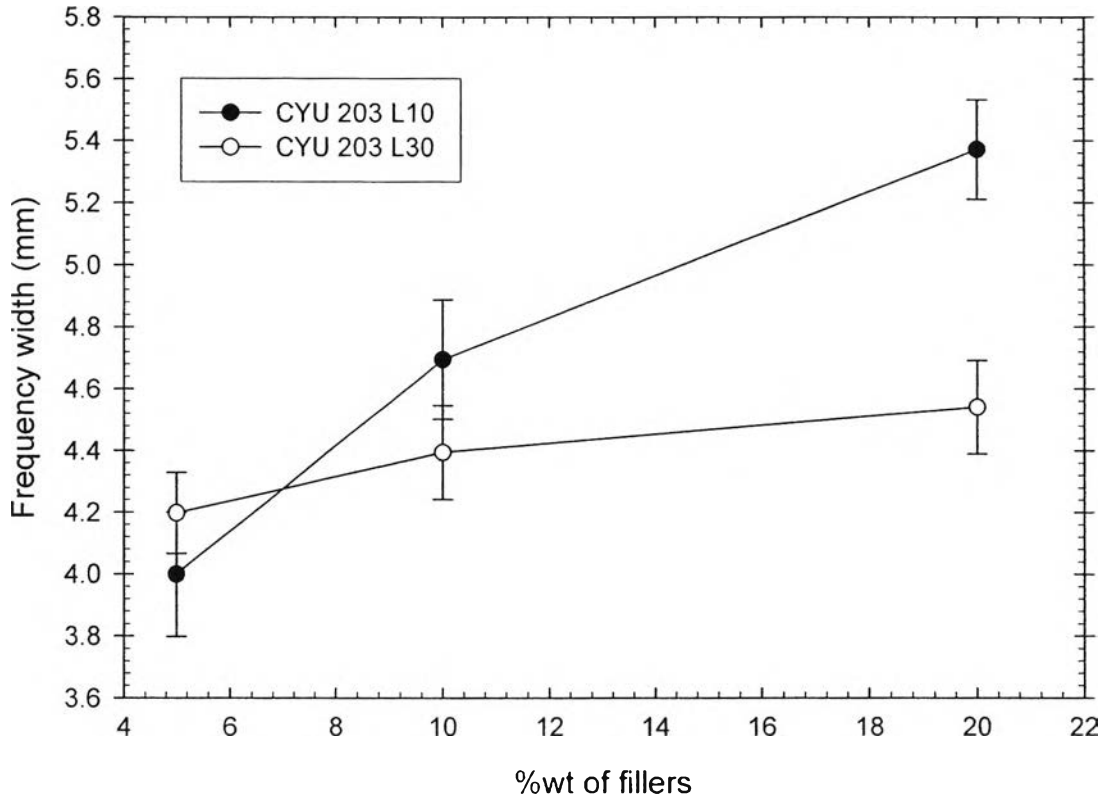
CYU 203 L10
CYU 203 L30
Frequency width (mm)
%wt of fillers
5.8
5.6
5.4
5.2
5.0
4.8
4.6
4.4
4.2
4.0
3.8
3.6
4
6
8
10
12
14
16
18
20
22

Fig. 7.16

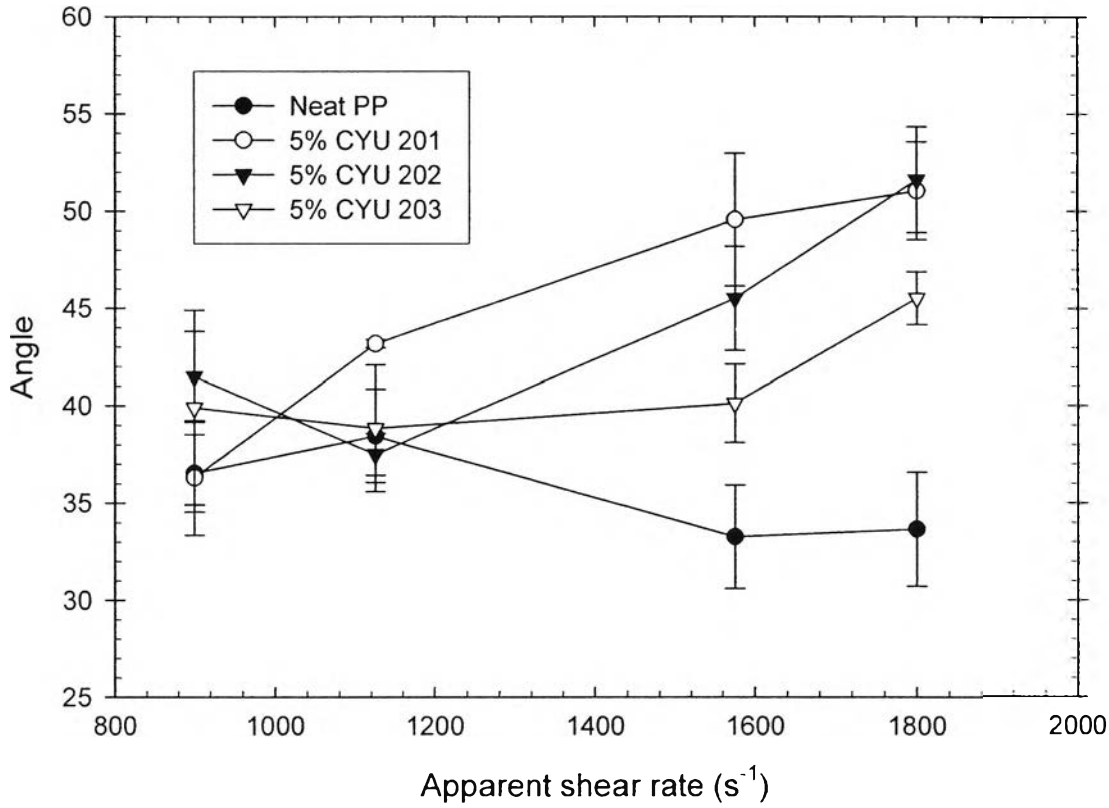
Neat PP
5% CYU 201
5% CYU 202
5% CYU 203
Angle
Apparent shear rate (s-1)
60
55
50
45
40
35
30
25
800
1000
1200
1400
1600
1800
2000

Fig. 7.17

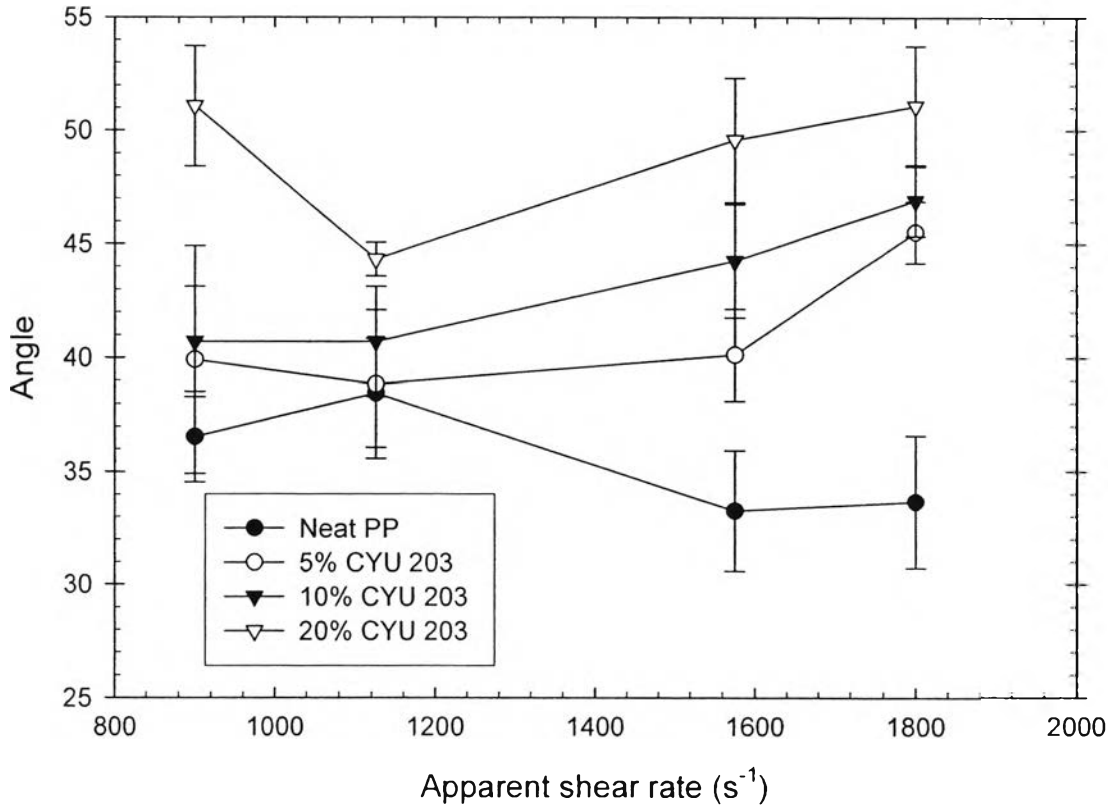
55
50
45
40
35
30
25
Angle
800
1000
1200
1400
1600
1800
2000
Apparent shear rate (s-1)
Neat PP
5% CYU 203
10% CYU 203
20% CYU 203

Fig. 7.18